
NUMERICAL MODEL OF TWO-PHASE FLOW IN CREUSOT-LOIRE UDDEHOLM (CLU) CONVERTER

¹T. Nyashanu, ¹G. Akdogan, ²R.H Eric and ³P. Taskinen

¹Department of Process Engineering, University of Stellenbosch, South Africa

²Department of Metallurgy and Materials, University of Witwatersrand, South Africa

e-mail: Rauf.Eric@wits.ac.za

³Department of Materials Science and Engineering, Aalto University, Finland

ABSTRACT

A two and three dimensional, transient and isothermal flow field of gas and liquid in a one-fifth scale bottom-blown Creusot-Loire Uddeholm (CLU) converter was simulated. Water and air were used to represent simulated matte and purged gas respectively. An Euler-Euler based algorithm was chosen for modelling fluid dynamics and evaluating controlling forces of a submerged gas injection. The calculation is based on the Reynolds Averaged Navier Stokes (RANS) equations. The VOF approach in conjunction with the realisable $k-\epsilon$ was used to solve the multiphase and transient nature of the flow respectively. The influence of gas flow rate and bath height on flow behaviour is discussed. Mixing time, which gives information on bath homogenisation was estimated and validated against the physical model. Predicted patterns of the flow field and the bulk phase velocity magnitudes were used to evaluate the general conditions inside the CLU. The bath height was varied from 0.5 m to 0.7 m and the gas flow rate was varied from 0.01 to 0.018 Nm³/s. The results show that the mixing time decreases with an increase in gas flow rate while increasing with an increase in bath height. The predicted mixing times agreed reasonably well with the published experimental data.

KEY WORDS: CLU converter, CFD model, isothermal, bottom-blowing, mixing efficiency.

1. BACKGROUND

Several metallurgical processes involve gas injection into liquid metals contained in a vessel, with a purpose to refine and homogenise the system under concern. Typical examples include degassing operations of molten steel by inert gas injection, desulphurisation of steel baths by inert carrier gases, and gas stirring ladles to achieve thermal and chemical homogeneity. Stainless steel production processes used today involve gas injection and comprise of two main stages, namely smelting and refining. Smelting of the charge such as scrap and process alloys occur in an electric arc furnace, which achieve highest energy densities and short meltdown times. Stainless steel refining includes a number of basic features such as decarburisation, deoxidation and desulphurisation. These operations are generally combined with alloying with the solid material. Carbon in stainless steel deteriorates oxidation resistance and welding characteristics and therefore its content needs to be reduced to specific low levels. Process conditions should allow decarburisation to occur without excessive loss of valuable metals such as nickel and chromium through oxidation. Carbon removal is favoured by high operating temperatures and low partial pressures of carbon monoxide in the molten bath. Columbus Stainless Steel in Middleburg utilises the Creusot Loire Uddeholm (CLU) converter for steel refining. The CLU converter is a large cylindrical vessel tapered at the bottom, with a capacity of 100 tonnes and operates at high temperatures between 1650°C and 1800°C. For the CLU process, superheated steam, oxygen and argon are injected into the converter through five submerged tuyeres arranged in an off-centre

configuration. Exchange of mass, momentum and heat between the bottom injections and the molten metal generates a vigorous advection in the molten bath. The bottom injections have a two-fold function which is to supply the oxidant for the excess carbon and also to agitate the bath. The injected gases supply energy to the bath in three forms, namely kinetic, buoyancy and expansion. This affects physical and chemical reactions occurring in the converter such as converting rate, oxygen efficiency, dispersion, mixing, heat and mass transfer, slopping, splashing and accretion growth (Valencia *et al.*, 2002). The resultant transport processes have a considerable effect on the thermal properties and cooling rates, which in turn strongly influence the quality of the final product. In order to increase the productivity of the steel refining process and to meet stringent quality standards, it is prerequisite to have a deeper insight on the process behaviour. However, due to high operating temperatures in steel refining and the large sizes of the metallurgical vessels, direct experimentation and observation are extremely difficult, if not impossible. It is against this background that researchers have resorted to scaled down physical and numerical models to analyse flow characteristics in metallurgical vessels. These macroscopic models provide a sound basis and may form a reliable predictive framework. These models have been found to be of substantial value in interpreting various process aspects such as reaction rates, refractory wear patterns and mixing characteristics (Cloete *et al.*, 2009).

One common approach to numerical modelling is Computational Fluid Dynamics (CFD). CFD is the science of finding solutions in space and time by solving numerically a set of fluid flow governing mathematical equations. Nowadays, CFD has become a powerful tool in predicting the performance of complex metallurgical processes. It is widely used to support new industrial plant developments, troubleshoot operational problems and to optimise industrial processes. The steady increase in computer power over the recent years has enabled researchers to model reaction multiphase flows. The cornerstone of the CFD software is the mixture of physical and numerical technologies that are used to solve governing transport equations (Johansen, 2003). As a result, the number of applications of CFD in metallurgical processes has not only grown rapidly, but also increased in sophistication.

A number of works have been done to study various flow phenomena in the CLU. Various reports in literature used physical models to elucidate the influence of various process parameters on the kinetics of submerged gas injection into the CLU (Eric, 2008) (Nyoka *et al.*, 2003) (Akdogan and Eric, 1999) (Kabezya and Eric, 2007). These researchers, *inter alia*, conducted physical modelling work that directly focused on the CLU. Akdogan and Eric (1999) studied mixing phenomena in a flat bottomed CLU model using pH measurement technique. The process of mixing in the CLU was also studied using a one-fifth scale mock-up water bath with five bottom nozzles (Nyoka *et al.*, 2003). These researchers proposed correlations for estimation of mixing times. Kabezya and Eric (2007) investigated the effect of gas flow rates and slag layer thickness on dispersion behaviour in the CLU. The results obtained revealed that the dispersed phase hold-up increased with increasing gas flow rate. Eric (2008) investigated CLU bath dynamics and inferred that mixing and mass transfer depends on gas flow rate, bath height and nozzle configuration. He deduced that mass transfer rates can be effectively controlled by varying tuyere configuration and gas flow rate at constant bath height. However, all the studies done to date on the CLU used only physical modelling to characterise the CLU process. The literature provides no numerical modelling to validate the results obtained from physical experiments. Although the CLU has been operational for more than three decades, there still remain some operational challenges, which lower considerably the productivity of the process. The major problems affecting the CLU operation are inadequate mixing and bath inhomogeneity that cause steel solidification on the reactor walls. Inefficient mixing leads to longer blowing periods which adversely affects the process economy (Eric, 2008). Owing to the vigorous nature of gas injection operations in the CLU converter, there is still no clear understanding of the actual bath dynamics, in particular fragmentation and coalition of

the rising bubbles, identification of dead volumes, and dissolution of solids in the bath. In order to solve the aforementioned operational challenges, a fundamental understanding of the CLU bath hydrodynamic behaviour during refining is prerequisite. Bath dynamics characterisation is therefore necessary to provide a platform for solving the CLU converter operational challenges and hence improve process productivity.

The current research sought to expand the knowledge of fluid flow inside the CLU converter and also to complement physical modelling done earlier on the CLU (Nyoka *et al.*, 2003). The study used CFD to formulate a computational model that depicts the flow phenomena in the CLU vessel. The influence of operating variables such as gas injection rate, vessel geometry, bath height and slag layer on bath dynamics, mixing and associated transport phenomena are studied numerically and validated against published experimental results. The objectives of the research project are to investigate the hydrodynamic behaviour of the CLU process using numerical modelling and to establish the effect of gas flow rates and bath height on mixing time and finally to validate the results against the findings of the physical model (Nyoka *et al.*, 2003).

2. NUMERICAL APPROACH

A transient and isothermal flow field in a one-fifth scale bottom-blown CLU was simulated. The flow problem setup was started with 2-D simulations consisting of simulated metal and simulated air only. Preliminary simulations were done by the author in order to build CFD capacity and also to familiarize with the pre-processing, processing and post-processing stages of ANSYS Fluent. The 2-D model was subsequently developed into 3-D. Mixing times were estimated using the inert tracer method. The methodology used in this numerical study was then validated by comparing the results to the physical model given in literature (Nyoka *et al.* 2003). Predicted patterns of the flow field and the bulk phase velocity magnitudes were used to characterize flow conditions inside the CLU. The bath height was varied within the range of 0.5 m to 0.7 m and the gas flow rate was varied from 0.01 m³/s to 0.0183 m³/s.

2.1. Computational Domain

The commercial CLU converter is a large cylindrical vessel with a capacity of 100 tons. It is tapered and is equipped with a step at the bottom. Figure 1 depicts a sketch of the one-fifth scale model used in this research which has five submerged nozzles arranged in an off-centre configuration as shown.

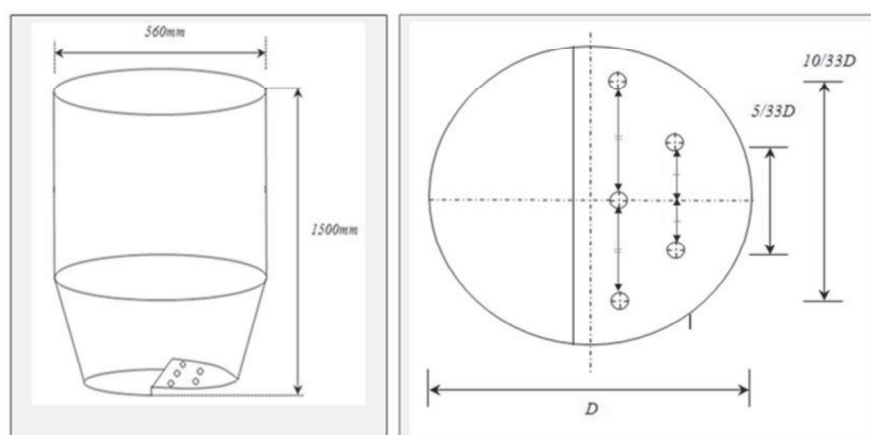


Figure 1: Schematic of the CLU model and the nozzle configuration

The pre-processing stage entailed geometry development and subsequent meshing in a commercial package called ANSYS Workbench that accompanies Fluent. The 2-D and 3-D schematics of the CLU model are depicted in figure 2.

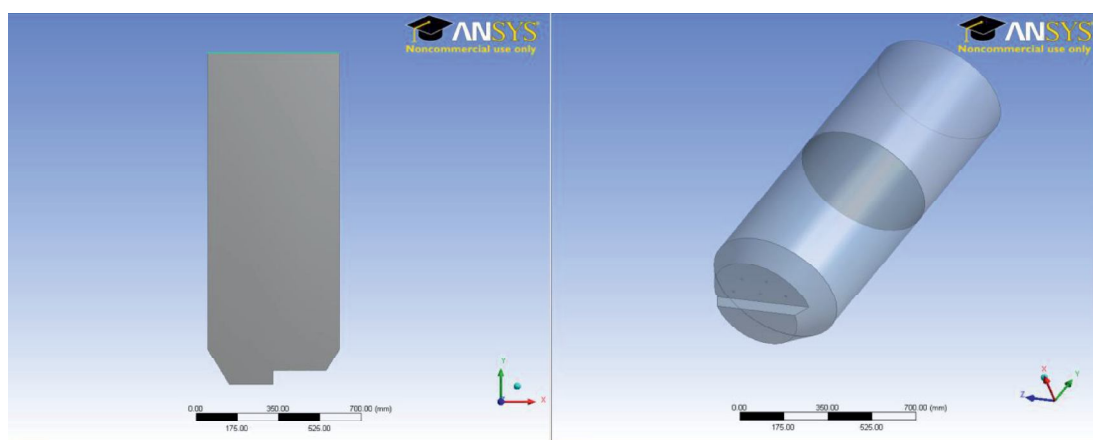


Figure 2

Details for the industrial prototype and the model are also highlighted in table 1.

Table 1: Comparative data for model and industrial prototype

| Parameter | Industrial Vessel | Model Vessel |
|-------------------|-------------------------------|---------------------------------|
| Liquid | steel | water |
| Nozzle diameter | 30mm | 6mm |
| Bath height | 2.9m | 0.5 – 0.7m |
| Froude Number | 242 | 242 |
| Purging gas | Steam/Argon/Nitrogen | Air |
| Gas purge rate | 0.93 to 1.69m ³ /s | 0.01 to 0.0183m ³ /s |
| Vessel material | Steel and refractory | Clear 6mm PVC |
| Number of nozzles | 5 | 5 |

2.2. Meshing

The computational domain was subdivided into a discrete and finite number of smaller and non-overlapping finite control volumes. For 2-D geometry, quadrilateral dominant type method was used with Quad/tri as the free face mesh type. An element size of 3mm was used in the region containing fluid while 10 mm was used for the empty region above the fluid region. A schematic for the 2-D mesh scheme is shown in figure 3. For the 3-D geometry, since the fluid flow in the domain is predominantly along the axis of the converter and the geometry is relatively simple, the hexahedral cell was chosen as the meshing element. Consequently, the problem was modelled with fewer grid cells, thus saving computational time and ensuring that numerical diffusion is minimised since the flow is aligned with the mesh. The quality of the mesh plays a significant role in the accuracy and stability of the numerical computation. Unstructured grid tetrahedral mesh elements were avoided since they are susceptible to numerical diffusion and need higher storage capacity. The generated mesh for the bottom section of the converter is also depicted in figure 3 and the total number of mesh cells for the whole geometry was about 120 000. A relatively fine mesh size of 4mm was used in the high gradient zones e.g. in the vicinity of the tuyere region while a relatively coarse mesh of size 20 mm was used for the gas phase above the liquid region. The main areas of

interest during the simulation included the interfaces of the different phases, high velocity plume regions, especially within the vicinity of the tuyere regions. These areas were resolved with a finer grid resolution that was adequate enough to capture the finer flow details. In this work, the computational cell skewness is used as the mesh quality measurement criterion. This measures the differences between the shape of the cell and the shape of an equilateral of equivalent area, both in 2-D and 3-D. For both the 2-D and 3-D computational domains used in the current study, the computational cells had greater than 94 % of the elements with an Equisize skew of 0.4 showing a good mesh quality.

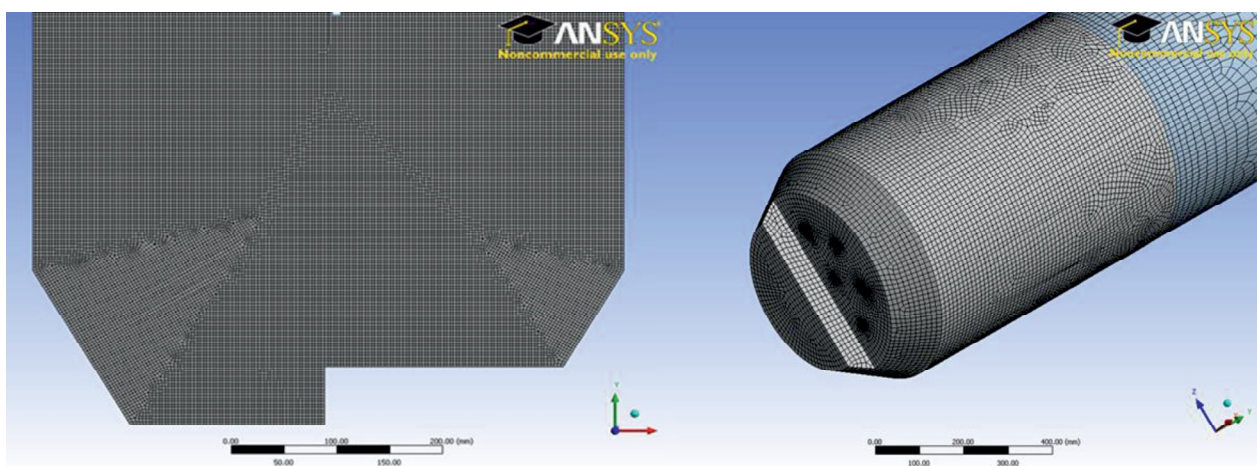


Figure 3: Schematic of the 2-D and 3-D mesh scheme

2.3. Mathematical Formulation and Method of Solution

Due to the complex nature of the flow phenomena in high strength agitated vessels, it is not possible to obtain a comprehensive solution of the flow field. Experimental observation were numerically studied on a 1.86GHz Intel(R) Core(TM)2 processor with 2GB RAM. A commercial code FLUENT was used and the calculation was based on the Reynolds Averaged Navier-Stokes (RANS) equations. The following assumptions were made into a statement of the mathematical model of the CLU model as: gas flow is single phase; temperatures inside the walls of the computing domain are constant; the free surface at the water-air interface is frictionless and flat; allowance is made for the escape of bubbles; an interface friction coefficient is used to describe the force between the liquid and the gas phase. Conservation of mass and momentum equations were used together with the species transfer equation to track the inert tracer through the domain, while neglecting all chemical reactions. The Volume of Fluid (VOF) approach and the realisable k- ϵ model were used to solve the multiphase and the turbulent nature of the flow respectively. During the calculation, the converged solutions were achieved when all the residuals for the partial differential equations were less than 0.001. The volume flux across the face was calculated using the Geometric Reconstruction scheme, which represents the interface between fluids using a piecewise-linear approach. This scheme is the most accurate and is applicable for general unstructured meshes. It assumes that the interface between the two fluids has a linear slope within each cell and uses a linear shape for the calculation of the advection of fluid through the cell faces. A time step of 0.0005 seconds was used for 3-D simulations. This time step was found to be sufficient for the achievement of numerical convergence and also maintain stability. For 2-D simulations, a time step of 0.001s was used and animation files were saved to qualitatively observe the behaviour of the rising plumes. A pressure based solver and a transient solution mode were used.

In order to obtain a solution in the domain, the partial differential equations used were discretised into algebraic equations for each computational cell. During the initial experiments, the first order discretisation scheme was used. This scheme simply assigns cell face values as equal to the value at the centroid. A second order discretisation scheme with stronger under-relaxation factors was later adopted to improve the accuracy of the solution. This scheme computes different cell face and centroid values and guarantees high accuracy of the solution with adequate stability. Pressure discretisation was done using PRESTO! Scheme which is recommended for swirl and strong streamlines. The power law was used for species discretisation. For pressure coupling, the PISO scheme was used. This scheme is part of the SIMPLE family of algorithms but completes additional iterations for skewness and neighbour corrections. Convergence was judged by means of scaled residuals of flow variables. A convergence criterion for $<10^{-3}$ for all the remaining variables was found to be sufficiently accurate.

2.4. Computation of mixing time

The inert tracer method was used to compute mixing times. After patching in the respective phases for a given simulation, the transient simulation was allowed to run until quasi steady state flow conditions were obtained. This condition was identified by monitoring the average flow velocity and also turbulent kinetic energy inside the vessel. Upon the monitored flow variables reaching a constant value, a volume of tracer was patched in the position as depicted in figure 4. The tracer was assigned material properties exactly the same as those of water (simulated metal) and was set up into a mixture with water. A VOF model comprising of air and the species mixture (water and tracer) was also set up. After initializing the solution, a section is patched inside the water region to contain the tracer material and another region is adapted for tracer mass fraction detection. The tracer addition and detection regions shown in figure 4 correspond exactly to the experimental set up reported in literature (Nyoka et al, 2003). Mixing time (T_{mix}) is defined as the time interval from the introduction of the tracer into the model to the point when the mass fraction of the tracer reaches a steady state value within $\pm 5\%$. It is the time required to attain phase equilibrium. From the species transfer equation, water was chosen as the n th species as it is the species with the larger mass fraction. This reduces modelling errors. The mass fraction of the tracer was chosen as one minus the mass fraction of water.

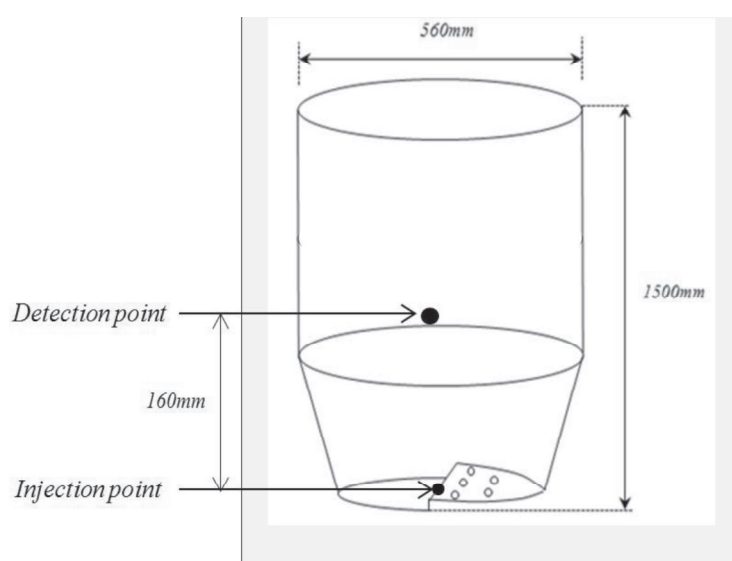


Figure 4: Schematic for inert tracer injection and detection

3. RESULTS AND DISCUSSION

The objective of this work was to characterise the flow behaviour in the CLU converter model and to investigate the influence of gas flow rates and bath height on mixing in the vessel. The results from the numerical model were also used to validate the physical model results published in literature.

3.1. Transient flow characteristics

Despite the flow calculations being conducted at different gas flow rates and bath heights, the flow behaviour in the vessel invariably depicted the same basic features. Given its buoyancy, the injected gas rose to the free surface inducing a turbulent recirculatory flow of the bath. The gas exiting from the nozzles formed a plume zone by exchanging momentum with the surrounding liquid and penetrated a certain distance into the bath before breaking into a swarm of rising bubbles.

The general plume structure in the vessel is shown by the contours of phase distribution through a vertical plane at different flow times as depicted in figure 5. As can be seen, the rising plume imparted turbulent kinetic energy and induced high turbulence to the surrounding fluid. It gradually became deflected towards the side wall on the right and this culminated into a circulatory motion in the bath. As the vertical distance from the nozzle region increased, the entrainment process increased the mass flow rate and the plume diameter while the plume axial velocity decreased. The flow details in figure 5 were captured at arbitrary flow time of 5s. The bath height was 0.7m and a gas flow rate of $0.0167 \text{ m}^3/\text{s}$ was considered.

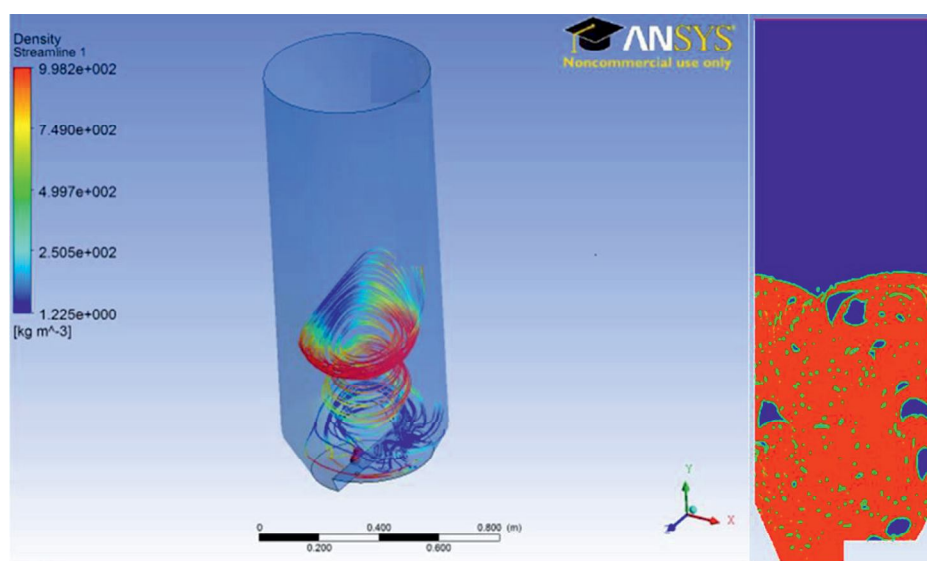


Figure 5: Plume structure and streamlines showing the rising plume in the CLU

The recirculating fluid flow pattern induced by the rising plume is important because of its metallurgical implications. The recirculatory fluid motion is well known for enhancing the rate of chemical and thermal homogenisation, as well as accelerating the absorption and floatation of harmful non-metallic inclusions into the overlaying slag phase through generation of turbulence. The gas plume also facilitates inclusion agglomeration and float out. The plume region displayed high turbulence and a large volume fraction of the gas. The high gas volume fraction in the plume region means that there are high oxidation rates of the metal in the recirculatory flows. Due to the recirculatory motion, freshly discharged gas mixes with the recirculatory flow of the metal near the

nozzle region. This means that most oxidation occur within the vicinity of the nozzle region during bubble fragmentation.

3.2. Bulk velocity profile

As can be seen in figure 6, the bulk velocities are high in the plume region and in the vicinity of the nozzle region. The recirculating fluid motion is however slow in the vicinity of the vessel bottom, forming distinct pockets of slowly moving fluid regions. It can therefore be inferred that mixing is more rapid in the plume regions and close to the free surface, whereas towards the base of the vessel, mixing becomes sluggish and distinct pockets of dead zones form at the base further from the nozzle region.

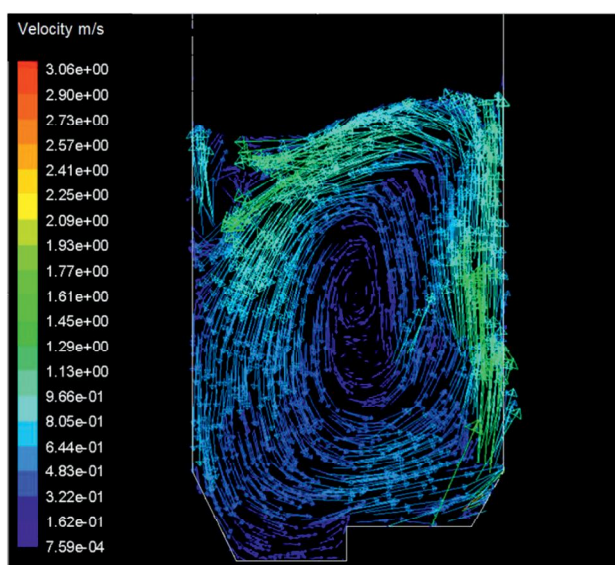


Figure 6: Velocity profile at 0.7 m bath height and 0.0167 m³/s

3.3. Two-phase model: Mixing time

A typical mixing time curve obtained from the simulations is given in figure 7. The tracer concentration in the detection zone increased gradually until it was within $\pm 5\%$ of a steady concentration value.

3.3.1. The effect of gas flow rate

As can be seen from figure 8, at a constant bath height, the mixing time decreased with an increase in the gas flow rate. When the gas flow velocity is increased, the centreline plume velocity increases resulting in rapid recirculation, which enhances mixing. At lower gas flow rates, the plume consisted of well-defined individual bubbles with less interaction. As the gas flow rate increased, there was more bubble interaction accompanied by vigorous advection in the bath. Further increase in the gas velocity changed the flow patterns, causing intermittent channelling of the gas through the bath. The results obtained from numerical simulations on the effect of gas flow rate are consistent with the earlier findings available in literature. Akdogan and Eric (1999) observed that at constant bath height, an increase in gas purge rate results in rapid circulation in the bath that results in rapid mixing.

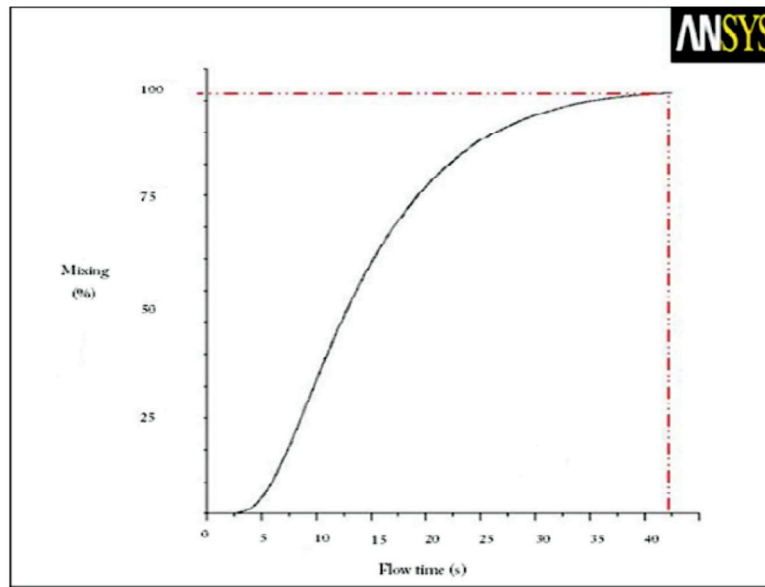


Figure 7: Typical mixing time result at 0.5 m bath height and 0.0127 m³/s

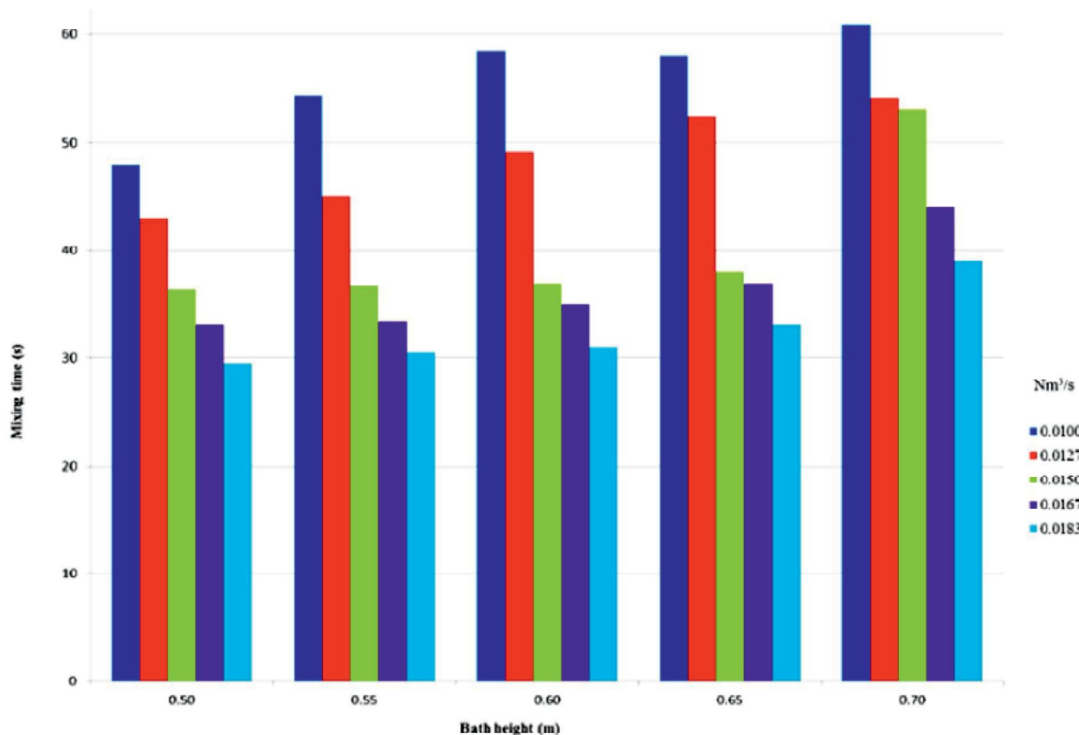


Figure 8: Variation of mixing times with gas flow rate at different bath heights

Eric (2008) observed that increasing the gas velocity also increases the cone angle. This increased the plume radius at the surface, effectively increased volume of the plume in the bath, and enhanced bath circulation. Sano et al. (1983) also studied the plume behaviour and concluded that

the increase in velocity is responsible for plume expansion and higher mixing intensity in the vessel. Another notable feature from the simulation results was the change in the trend behaviour which seemed to suggest that a gas flow rate of $0.0155 \text{ m}^3/\text{s}$ was the critical gas flow rate. Figure 9 depicts the variation of mixing time with gas flow rate.

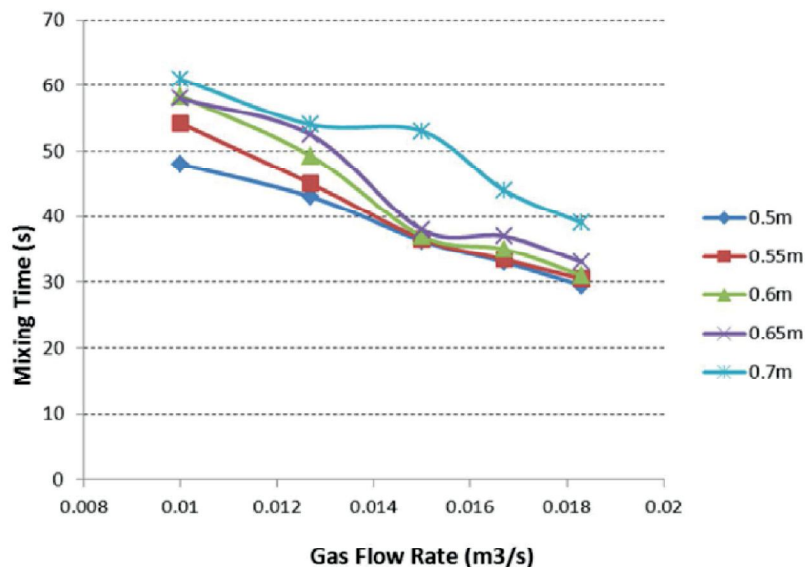


Figure 9: Variation of mixing time with gas flow rate

The mixing times decreased sharply with an increase in gas flow rate up to a value of $0.0155 \text{ m}^3/\text{s}$. This is due to increased bubble interaction in the vessel. However, beyond this value, the mixing times attained an upward trend before decreasing once more. Beyond $0.0155 \text{ m}^3/\text{s}$ is characterised by channelling, especially at higher bath heights of 0.65 m and 0.7 m. Akdogan and Eric (1999) suggested that beyond the critical gas injection rate, any further increase in plume radius slows down plume velocity by radial propagation of the velocity component all along the plume to the surface. This adversely influences bath recirculation.

3.3.2. Effect of bath height

At all gas flow rates, the mixing times increased with an increase in bath height. At smaller bath heights, the flow comprised of smooth circulatory flow patterns which filled the entire vessel. However, as the bath height was increased, dead zones became predominant in the vessel, especially at the bottom end of the vessel further from the nozzle region. The presence of dead zones resulted in extended mixing times. This is depicted in figure 10.

Sano et al. (1983) reported a reduction in plume size with an increase in bath height as a major factor leading to the extension of mixing times. In their investigation, Mazumdar and Guthrie (1985) found out that interference of the plume with the recirculatory flow and also sharp angles on the bath geometry led to the formation of dead zones in the vessel. Krishnamurthy et al. (1988) explained the increase in mixing times at higher bath heights by means of a circulation model in which the bath consists of cells that hinder mixing by bulk circulation. Nyoka et al. (2003) associated this phenomenon to the reduction of bubble formation near the bottom of the vessel, especially on the stepped side. All these arguments raised by different researchers concur with the current CFD simulation results.

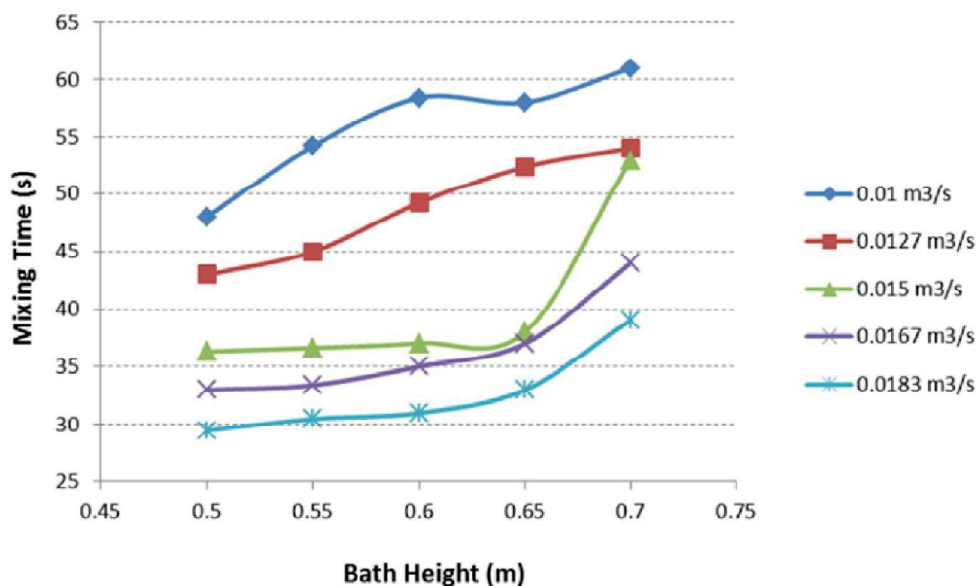


Figure 10: Variation of mixing times with bath height

3.3.3 Validation of predicted results

The numerical mixing results for a two-phase 3-D model were validated against published experimental results (Nyoka et al., 2003). Table 2 shows a comparative analysis of the physical and numerical results.

For all various process parameters tested, there was a good agreement between the numerical and physical results. The predicted mixing times showed the same trend of variation as those obtained from the physical model. A percentage Absolute Average Deviation from the physical experiment is computed for each set of data. The data exhibited reasonably low values of the AAD value (average of 10.6%) and the graphical profiles of both experimental and model predictions matched in trends and small deviations between experimental and numerical results can be explained in terms of experimental errors and also computational errors arising from meshing and discretisation methods. Nevertheless, it was found that there exists a good agreement between the numerical and physical results. This suggested that the assumptions adopted in the mathematical model did not have any noticeable impact on the calculated overall momentum transport between phases. A good agreement between numerical and physical results confirms that CFD is a reliable tool that can be used for predicting multiphase fluid flow phenomena.

4. CONCLUSIONS

In this study, a transient, turbulent and isothermal flow field of gas and liquid phases in a one-fifth scale CLU has been simulated using the Eulerian method. The influence of the gas flow rate and bath height on the mixing in the vessel has been investigated. Mixing times, which give information on bath homogenisation were estimated and validated against the physical model in order to verify the efficacy of the numerical model. An analysis of flow patterns, plume morphology and structure was done. According to the results, the following conclusions can be drawn: the observed bath dynamics showed that the injected gas from the off-centred tuyeres ascends and is gradually deflected towards the right sidewalls (close to the nozzle region).

Table 2: Comparative analysis for numerical and physical results

| Bath height, m | Gas flow rate, Nm ³ /s | Mixing time, s | |
|----------------|-----------------------------------|----------------|-----------------------------------|
| | | Numerical | Experimental (Nyoka et al., 2003) |
| 0.5 | 0.010 | 48.00 | 54.44 |
| | 0.0127 | 43.00 | 48.71 |
| | 0.015 | 36.30 | 39.25 |
| | 0.0167 | 33.00 | 31.88 |
| | 0.0183 | 29.50 | 35.90 |
| 0.55 | 0.010 | 54.20 | 58.25 |
| | 0.0127 | 45.00 | 48.00 |
| | 0.015 | 36.60 | 39.00 |
| | 0.0167 | 33.40 | 35.10 |
| | 0.0183 | 30.50 | 32.56 |
| 0.60 | 0.010 | 58.40 | 65.20 |
| | 0.0127 | 49.20 | 55.20 |
| | 0.015 | 37.00 | 38.75 |
| | 0.0167 | 35.00 | 40.89 |
| | 0.0183 | 31.00 | 32.78 |
| 0.65 | 0.010 | 58.00 | 60.89 |
| | 0.0127 | 52.40 | 47.00 |
| | 0.015 | 38.00 | 38.75 |
| | 0.0167 | 37.00 | 43.13 |
| | 0.0183 | 33.00 | 42.00 |
| 0.70 | 0.010 | 61.00 | 75.30 |
| | 0.0127 | 54.00 | 39.33 |
| | 0.015 | 53.00 | 58.86 |
| | 0.0167 | 44.00 | 48.20 |
| | 0.0183 | 39.00 | 43.44 |

This culminates into a recirculatory flow pattern which is ideal for high mixing efficiency in the bath. At a constant bath height, mixing time decreases with an increase in gas flow rate due to an increase in the centreline plume velocity which results in rapid bath circulation and hence higher mixing intensity. At a constant gas flow rate, mixing time decreases with an increase in bath height. This is due to the formation of dead zones and reduction in plume size at higher bath heights. There was a good agreement between the numerical results and those obtained from the physical experiments. It can therefore be concluded that CFD is a reliable tool for the prediction of multiphase fluid flow behaviour in metallurgical vessels.

5. REFERENCES

- [1] Akdogan,G., Eric, R.H., (1999) Model study on dispersed phase hold up in ferroalloy refining processes, Fluid Flow phenomena in Metal Processing, TMS Annual Meeting, San Diego, USA, Ed by El Kaddah, DGC Robertson, S. T. Johansen, and V. R. Voller, pp. 117-125.
- [2] Akdogan,G., Eric, R. H., (1999) Model study on Mixing and Mass transfer in Ferroalloy refining processes, Metallurgical and Materials transaction B, vol. 30B, No. 2, pp. 231- 239.

- [3] Cloete, S., Eksteen, J.J., Bradshaw, S. M., (2009) A mathematical modelling study of fluid flow and mixing in full scale gas stirred ladles. *Progress in Computational Fluid Dynamics*, Vol 9, No. 6, 345-356.
- [4] Eric, R.H., 2008. Physical Modeling of Ferroalloy/Stainless Steel Refining Reactors, *International Journal of Materials and Manufacturing Processes* , 23(8), 764-768.
- [5] Johansen, S. T., (2003) Mathematical modelling of metallurgical processes, Paper presented at the Third International Conference on CFD in the Mineral and Process Industries, Melbourne, Australia, 10-12 December.
- [6] Kabezya, K. and Eric, R., (2008) Study of dispersion phenomena in Creusot Loire Uddeholm reactor, *Minerals Engineering*, 21(2), pp. 138-142.
- [7] Krishnamurthy G. G., Mehrotra, S. P., and Gosh A., (1988) *Metall Trans. B.*, Vol. 19B, pp. 839-850.
- [8] Mazumdar, D. and Guthrie R. I. L., (1985) Hydrodynamic of some gas injection procedures in ladle metallurgy operations, *Metall. Trans. B.* 16B, pp. 83-90.
- [9] Nyoka, M., Akdogan, G., Eric, R. and Sutcliffe, N., (2003) Mixing and solid-liquid mass-transfer rates in a Creusot-Loire Uddeholm vessel: A water model case study. *Metallurgical and Materials Transactions B*, 34(6), pp. 833-842.
- [10] Sano, M. and Mori, K., (1983) Scaninjet III, Part 1, Lulea, Sweden, No. 6, Vol. 23, pp. 43-50.
- [11] Valencia, A., Cordova, M., Ortega, J., (2002) Numerical simulation of gas bubbles formation at submerged orifice in a liquid, *International Conference on Heat and Mass Transfer*, Vol. 29, No. 6, pp. 821-830.

